

# Quantum Fisher Information of Three-Level Atom Under the Combined Influence of the Non-Linear Kerr Medium and the Stark Effect

Syed Jamal Anwar\*, Ibrahim M, & Khalid Khan

Department of Physics, Quaid-i-Azam University, Islamabad

\*Corresponding author: Syed Jamal Anwar, Department of Physics, Quaid-i-Azam University, Islamabad.

Submitted: 07 April 2025 Accepted: 14 April 2025 Published: 21 April 2025

doi <https://doi.org/10.63620/MKSSJP.2025.1052>

**Citation:** Anwar, S. J., Ibrahim, M., & Khan, K. (2025). Quantum Fisher Information of Three-Level Atom Under the Combined Influence of the Non-Linear Kerr Medium and the Stark Effect. *Sci Set J of Physics*, 4(2), 01-09.

## Abstract

We explore the dynamics of Quantum Fisher Information (QFI) and Von Neumann Entropy (VNE) in three-level stationary and moving Stark-shifted atomic systems influenced by a Nonlinear Kerr Medium (NLKM). QFI, which measures coherence and sensitivity to parameter changes, decreases over time due to decoherence, with slower decay at higher nonlinearity values. VNE, an indicator of quantum entanglement, increases over time, with stronger growth observed at lower nonlinearity value. The Stark effect, caused by an external electric field, introduces energy level shifts that result in oscillatory behavior in both QFI and VNE. Stronger electric fields amplify these oscillations, enhancing sensitivity and entanglement dynamics. The system's phase significantly impacts its behavior, with symmetric patterns emerging at zero phase and more complex dynamics occurring at other phase values.

In moving systems, atomic motion interacts with NLKM and Stark effects to produce periodic modulations in QFI and VNE. Lower nonlinearity values lead to pronounced oscillations, reflecting stronger quantum interactions, while higher values stabilize coherence. Peaks in QFI often align with dips in VNE, indicating a trade-off between precision and entanglement. Transient spikes in VNE highlight moments of enhanced quantum entanglement, while high QFI values signify robust coherence, critical for precision measurements. This study demonstrates the tunability of quantum systems through external field strength, nonlinearity, and phase, providing a framework for optimizing quantum sensing and exploring the fundamental dynamics of coherence and entanglement in quantum systems.

**Keywords:** Quantum Entanglement (QE), Quantum Fisher Information (QFI), Stark Effect (SE), von Neumann entropy (VNE), Non-Linear Kerr Medium (NLKM)

## Introduction

The interaction between a two-level atom and a single quantized mode of a radiation field, within the framework of the rotating wave approximation (RWA), is commonly referred to as the Jaynes-Cummings model (JCM) [1]. This model describes the cyclic process of photon absorption and emission by the atom, which enables energy and momentum transfer between the atom and the radiation field. Studying the JCM provides valuable insights into the dynamics of atom-field interactions. The JCM has been the subject of extensive theoretical [2] and experimental investigations [3]. Over the past few decades, quantum optics

research has increasingly focused on three-level systems interacting with one- or two-mode cavity fields in various configurations. Yoo and Eberly conducted in-depth studies of three-level atoms in different configurations interacting with quantized fields under RWA in an ideal cavity [4].

A generalized framework for the JCM, involving three-level atoms interacting with one- or two-mode non-resonant cavity fields, has also been established [5]. Additional studies have examined three-level systems under multi-photon interactions, systems with field-dependent coupling constants, NLKM and

interactions involving non-correlated two-mode fields [6-10]. Recent advancements include the application of the modified homotopy analysis method to obtain the wave function of a three-level atom and the derivation of a general solution for such systems in the presence of gravity [11, 12]. Other areas of interest include analyzing atomic motion in the JCM, investigating the dynamics of entanglement in three-level atoms, and studying interactions between a three-level atom in a momentum eigenstate and a one-mode cavity field within a NLKM [13-15]. Furthermore, alternative Lie algebra  $SU(3)$  approaches have been employed to explore the internal and external dynamics of a three-level atom interacting with a one-mode cavity field under the influence of an atomic gravity field [16].

When particles are separated by a certain distance, they can exhibit a remarkable connection that persists regardless of the physical separation between them. This phenomenon, known as QE, allows the state of one particle to instantaneously affect the state of another, even when they are far apart [17-20]. In real-world quantum systems, open quantum structures are critical to consider. These systems interact with their environment and are influenced by external conditions, making them highly relevant in understanding entanglement dynamics. However, such interactions often lead to detrimental effects, including a process known as decoherence. Decoherence refers to the degradation of coherence or entanglement within the system, which ultimately results in the loss of quantum information [21-23].

To fully comprehend the impact of environmental factors on quantum information, it is vital to evaluate the parameters of a quantum system both before and after its interaction with a noisy channel. This evaluation process, known as quantum metrology, focuses on utilizing quantum principles to enhance measurement precision [24, 25]. Quantum metrology encompasses various techniques, such as the Quantum Cramer-Rao Bound, QFI, Heisenberg-Limit Metrology, and Time-Evolution-Based Metrology. Among these, QFI serves as a foundational metric for determining the precision of parameter estimation in quantum systems, highlighting its versatility in comparing different metrological methods [26].

QFI plays a pivotal role in quantum metrology by defining the theoretical limits of parameter estimation precision for quantum states. While much research has been devoted to exploring QFI independently of noisy environments [27, 28], the substantial influence of dissipative processes—prevalent in real-world quantum systems—warrants significant attention. Dissipative channels, which induce decoherence and result in information loss, are particularly critical in this regard [29, 30]. Kraus operators offer a powerful mathematical framework for modeling open quantum systems, providing insights into how dissipative interactions modify quantum states and affect QFI [31]. This framework is essential for understanding the behavior of quantum systems in practical scenarios, where noisy and dissipative environments are unavoidable.

The Kerr effect refers to the phenomenon where the refractive index of a material changes in response to an applied electric field, leading to a nonlinear optical effect. When combined with quantum entanglement, the Kerr effect can be used to create and manipulate entangled states [32]. For instance, in an optome-

chanical system, the Kerr effect can enhance the entanglement between light and mechanical oscillators [33]. The Stark effect occurs when an external electric field causes a shift and splitting of atomic or molecular energy levels [34]. This effect can be used in quantum information processing to control and generate entangled states [35]. For example, the dynamic Stark effect can be employed to generate entanglement between photons and atoms in a laser-driven quantum optical system [36].

The goal of our current investigation is to determine the QE dynamics of a three-level atomic system under the influence of the SE and NLKM, considering both the presence and absence of a moving atom. Our motivation lies in examining how these effects impact QE. We investigate how both the NLKM and SE simultaneously affect the dynamics of QFI and VNE in three-level atomic systems, considering both stationary and moving atoms.

It is evident the SS predominate during the quantum system's temporal growth. The SS significantly affects QFI dynamics. Furthermore, the SS affects the VNE more strongly when there is no motion of atom. VNE is a crucial concept in quantum statistical mechanics, where it helps describe the thermodynamic properties of quantum systems in equilibrium. It relates to concepts like temperature and free energy in the quantum context.

The structure of this document is organized as follows: Section 2 outlines the system model, focusing on a three-level atomic system influenced by a coherent field, incorporating the effects of SE and NLKM. This section also includes the model Hamiltonian and interaction dynamics. Section 3 presents a detailed discussion along with numerical results. Finally, Section 4 concludes with a concise summary of the findings.

### Hamiltonian Model

We study the system of moving 3-level atom interacting with coherent field in the presence of combined effect of the SE and NLKM we study the cascade configuration of the system. Assuming the RWA, the system  $H^A_T$ , is given by [37].

$$\hat{H}_T = \hat{H}_{Atom-Field} + \hat{H}_I. \quad (1)$$

where  $H_{Atom-Field}$  shows the atom which is not interacting and field Hamiltonian, and  $H_I$  represents the coupling portion. Our writing for  $H_{Atom-Field}$  will be

$$\hat{H}_{Atom-Field} = \sum_j \omega_j \hat{\sigma}_{j,j} + \nu \hat{a}^\dagger \hat{a}, \quad (2)$$

where the  $j$ th levels  $\sigma_{j,j} = |j\rangle\langle j|$  represents atomic population operator. atomic population operators, were essentially referring to the operators that describe transitions between different energy levels of the atom. These transitions play a crucial role in entanglement dynamics.

It depicts a two-level atom when  $N = 1$ , and the 3-, 4-, and 5-level atoms when  $N = 3, 4$ , and 5.

When it comes to SE and NLKM, the  $H^A_I$  is provided by

$$\hat{H}_I = \sum_{s=1}^3 \Omega(t) \left[ \hat{a} e^{-i\Delta_s t} \hat{\sigma}_{s,s+1} + (\hat{a} e^{-i\Delta_s t} \hat{\sigma}_{s,s+1})^\dagger \right] + \beta \hat{a}^\dagger \hat{a} + \chi \hat{a}^{\dagger 2} \hat{a}^2, \quad (3)$$

$\chi$  is the parameter of NLKM,  $\beta$  is the parameter of SE and the detuning parameter is described as

$$\Delta_s = \nu - (\omega_s - \omega_{s+1}). \quad (4)$$

The coupling constant between the atom and the field is denoted as  $g$ , while  $(t)$  represents the shape function of the cavity-field mode [37]. The atom's motion is assumed to occur along the  $z$ -axis for specific considerations of interest.

$(t) = g \sin(p\pi vt/L)$  in the presence of atomic motion,  $p \neq 0$

$(t) = g$  in the absence of atomic motion  $p = 0$  (5)

The velocity of the atom is represented by  $v$ ,  $p$  corresponds to half the number of wavelengths of the cavity mode, and  $L$  denotes the cavity's length along the  $z$ -direction. By setting the atom's velocity as  $v = gL/\nu$ , we arrive at the following result.

$$\Omega_1(t) = \int_0^t \Omega(\tau) d\tau = \frac{1}{p} (1 - \cos(p\pi vt/L)) \text{ for } p \neq 0 \quad (6)$$

$$= gt \text{ for } p = 0. \quad (7)$$

To achieve maximum precision in determining the phase shift parameter, the optimal input state is considered as follows

$$|\Psi(0)\rangle_{\text{Opt}} = \frac{1}{\sqrt{2}}(|1\rangle + |0\rangle) \otimes |\alpha\rangle. \quad (8)$$

Here,  $|1\rangle$  and  $|0\rangle$  represent the states of the atom, while  $\alpha$  denotes the coherent state of the input field, expressed as follows

$$|\alpha\rangle = \sum_{n=0}^{\infty} \alpha^n \sqrt{e^{-|\alpha|^2}/n!} |n\rangle \quad (9)$$

We analyze a phase gate that operates on a single atom and applies a phase shift

$$\hat{U}_\phi = |1\rangle\langle 1| + e^{i\phi} |0\rangle\langle 0|, \quad (10)$$

The state  $|\Psi(0)\rangle$  is derived by applying the single-atom phase gate to the initial optical state

$|\Psi(0)\rangle_{\text{Opt}}$

$$\hat{U}_\phi |\Psi(0)\rangle_{\text{Opt}} = |\Psi(0)\rangle \quad (11)$$

$$= \frac{1}{\sqrt{2}}(|1\rangle + e^{i\phi}|0\rangle) \otimes |\alpha\rangle \quad (12)$$

Following the phase gate operation, the system interacts with a field. In the time-independent scenario, the wave function is described using the transformation matrix  $U^\wedge(t)$

as expressed

$$|\Psi(t)\rangle = \hat{U}(t) |\Psi(0)\rangle \quad (13)$$

The density matrix (DM) can be explicitly expressed as

$$\hat{\rho}(t) = \sum_{m,n}^N |\Psi_n(t)\rangle \langle \Psi_n(t)| \hat{\rho}(0) |\Psi_m(t)\rangle \langle \Psi_m(t)| \quad (14)$$

In this manner, the QFI for a bipartite density operator  $\rho_{AB}$  can be defined with respect to, as described by [38].

$$I_{QF}(t) = I(\phi, t) = \text{Tr}[\rho_{AB}(\phi, t) \{L^2(\phi, t)\}], \quad (15)$$

here,  $L(\phi, t)$  represents the quantum score, also known as the symmetric logarithmic derivative (SLD), and can be determined as described by [39].

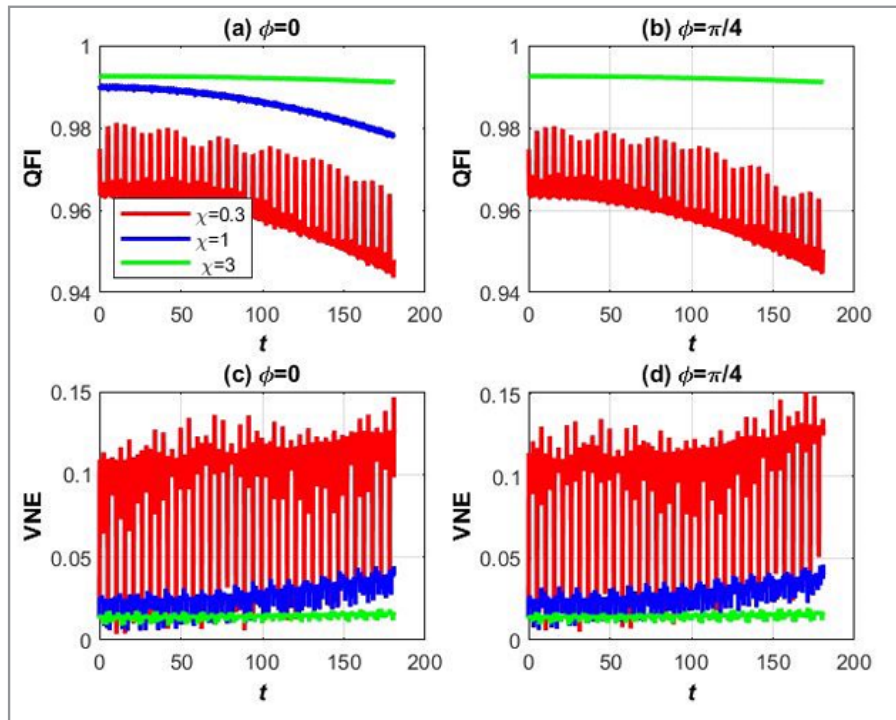
$$\frac{\partial \rho(\phi, t)}{\partial \phi} = \frac{1}{2} [L(\phi, t) \rho_{AB}(\phi, t) + \rho_{AB}(\phi, t) L(\phi, t)]. \quad (16)$$

Likewise, the VNE is described as

$$S_A = -\text{Tr}(\rho_A \ln \rho_A) = -\sum_i r_i \ln r_i, \quad (17)$$

where  $r_i$  represent eigenvalues of the atomic DM  $\rho_A = \text{Tr}_B(\rho_{AB})$ . The next section explores how various environmental parameters,  $p$ ,  $\chi$ , and  $\beta$  affect the evolution of the QFI and VNE.

We have done the numerical calculations as the system is bigger to solve analytically, we used computational languages and software for the numerical calculations. We have described clearly the Hamiltonian of the system and the interaction Hamiltonian. We also mention the state and also the formulas for QE quantifiers like QFI and VNE. To quantify QE, we construct the density matrix, and this density matrix is solved numerically. With the help of this density matrix Eigen vectors and Eigen values of the density matrix are calculated. These eigenvectors and eigenvalues are used to calculate QFI and VNE but this whole calculation is numerical.



The QFI (upper portion) and VNE (lower portion) vs time,  $\alpha = 6$ ,  $\beta = 0.3$  and  $\chi = 0.3, 1, 3$  and  $\phi = 0$  (left side) and  $\pi/4$  (right side),  $p = 0$ .

### Discussions and Numerical Outcomes

We consider both of the static and moving cases of the three-level system, and the presence of the coherent field. The systems level is SE with strength  $\beta$  in the presence of NLKM. We solve the system dynamics numerically and have chosen a 0.1-time step size.

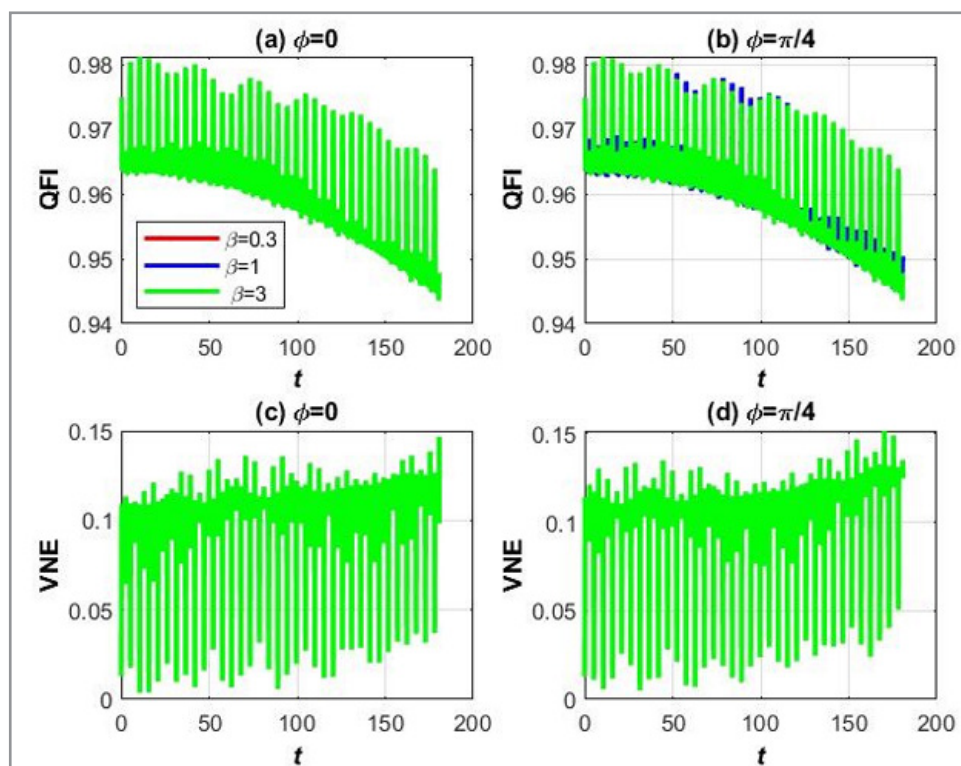


**Figure 1:** The QFI (upper portion) and VNE (lower portion) vs time,  $\alpha = 6$ ,  $\chi = 0.3$  and  $\beta = 0.3, 1, 3$  and  $\phi = 0$  (left side) and  $\pi/4$  (right side),  $p = 0$ .



## VNE and QFI of three- level stationary Stark Shifted atomic systems under the Influence of NLKM

### Explanation of the Graphs

Fig-1 QFI measures the information that an observable random variable carries about an unknown parameter, used to quantify the sensitivity of a quantum state to changes in a parameter. Subplots (a) and (b) show QFI versus time for two phase values:  $\phi = 0$  and  $\phi = \pi/4$ . Each curve represents different NLKM parameter values:  $\chi = 0.3$  (red), 1 (blue), and 3 (green). QFI decreases over

time for all 3 values, with a more pronounced decrease for lower  $\chi$  values. VNE quantifies the amount of quantum entanglement (QE) in a state. Subplots (c) and (d) show VNE versus time for the same phase values. Each curve represents different  $\chi$  values: 0.3 (red), 1 (blue), and 3 (green). VNE increases over time for all  $\chi$  values, with a more pronounced increase for lower  $\chi$  values. The Stark effect refers to the shifting and splitting of spectral lines due to an external electric field ( $\beta = 0.3$ ). NLKM parameter

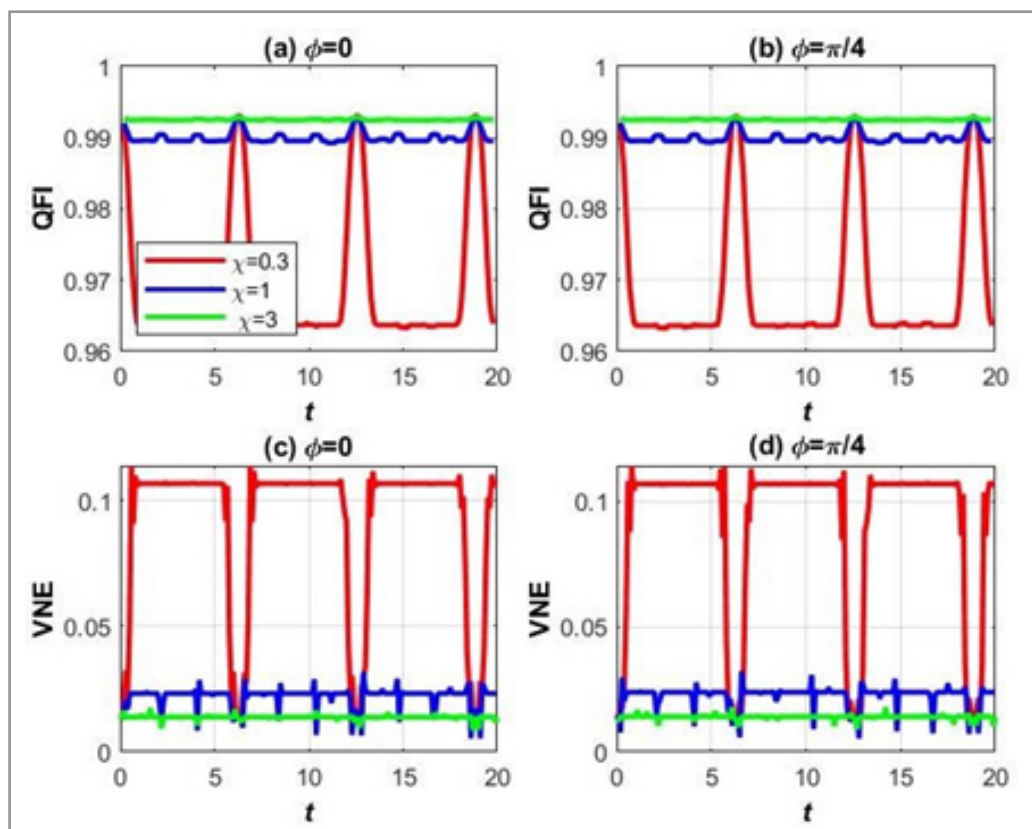


**Figure 2:** The QFI (upper portion) and VNE (lower portion) vs time,  $\beta = 0.3$  and  $\chi = 0.3, 1, 3$  and  $\phi = 0$  (left side) and  $\pi/4$  (right side),  $p = 1$ .

$\chi$  represents the strength of non-linear interaction. Lower  $\chi$  values lead to a higher increase in VNE, indicating stronger QE, while higher  $\chi$  values result in a slower increase, indicating weaker QE. QFI is crucial in quantum metrology for estimating a parameter, with higher QFI indicating more extractable information. Higher  $\chi$  values stabilize the quantum state against decoherence, slowing QFI decay over time. The Stark effect ( $\beta = 0.3$ ) influences energy levels and phases, affecting sensitivity to parameter changes. VNE measures the degree of entanglement. Lower  $\chi$  values enhance QE, leading to a steeper increase in VNE, while higher  $\chi$  values result in slower QE dynamics.

The applied electric field ( $\beta = 0.3$ ) shifts energy levels and alters phase, influencing entanglement generation and evolution by changing energy state interactions. QFI decreases over time due to decoherence, with a faster decrease for lower  $\chi$  values and a slower decrease for higher  $\chi$  values. VNE increases over time, indicating growing QE, with a faster increase for lower  $\chi$  values and a slower increase for higher  $\chi$  values. At  $t = 0$ , the initial phase doesn't introduce additional complex phases, and the decrease in QFI is driven by the systems intrinsic dynamics. At

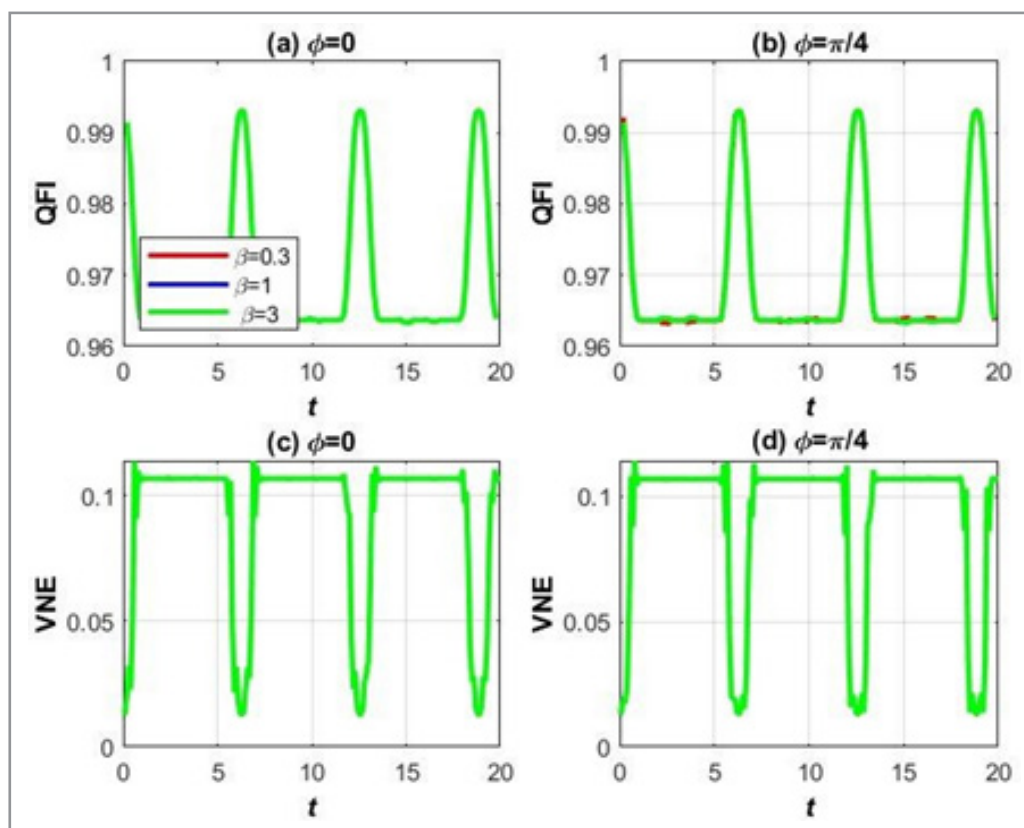


**Figure 3:** The QFI (upper portion) and VNE (lower portion) vs time,  $\chi = 6$ ,  $\phi = 0.3$  and  $\beta = 0.3, 1, 3$  and  $\phi = 0$  (left side) and  $\pi/4$  (right side),  $p = 1$ .

$\pi/4$ , additional phase shifts affect interference patterns and sensitivity. The Stark effect and NLKM interactions shape QE and information metrics, with phase introducing complexity into the system's evolution.

FIG-2 QFI measures the sensitivity of a quantum state to parameter changes and is crucial for quantum metrology. Higher QFI indicates better precision. VNE measures quantum entanglement (QE); higher VNE indicates more QE.

The Kerr effect is a nonlinear optical effect where a material's refractive index changes with light intensity. The parameter  $\chi$  represents this nonlinearity. The Stark effect refers to spectral line shifts due to an external electric field, with parameter  $\beta$  indicating its strength. Subplot (a)  $\phi = 0$ ,  $\beta = 0.3, 1$ , and  $3$ , QFI starts around  $0.98$  and decreases over time, with more significant fluctuations for higher  $\beta$ . Subplot (b)  $\phi = \pi/4$ : Similar to (a) but with a slightly more pronounced QFI decrease. Subplot (c)  $\phi = 0$ : VNE fluctuates around  $0.1$ , with larger fluctuations for higher  $\beta$ . Subplot (d)  $\phi = \pi/4$ : Similar to (c) but with slightly more pronounced fluctuations. The Stark effect leads to significant fluctuations in both QFI and VNE, indicating its impact on sensitivity and QE dynamics. This analysis helps understand how external fields and nonlinear effects influence precision and QE in quantum systems. QE, where particles remain connected regardless of distance, is vital for quantum computing and cryptography. QFI indicates how much information a quantum system carries

about a parameter. Entangled states generally have higher QFI, improving parameter estimation precision. In quantum metrology, entangled states achieve precision beyond classical limits. QE dynamics, influenced by external fields and nonlinear interactions, affect QFI.

VNE measures QE, with higher values indicating more entanglement. Nonlinearities and external fields cause QE to fluctuate, often correlating with QFI changes. Both QFI and VNE are linked to QE. High QFI often corresponds to high VNE. The Kerr nonlinearity and Stark effect modulate QE, causing fluctuations in both measures. Understanding these relationships optimizes quantum systems for quantum metrology and information processing. Graphs show QFI and VNE varying over time and with different  $\beta$  values. Higher  $\beta$  results in more significant QFI and VNE changes, indicating stronger external fields enhance QE and sensitivity. Utilizing highly entangled states with high QFI allows precision measurements beyond classical limits. Analyzing QE and sensitivity changes with external parameters tailor's quantum systems for specific tasks.

### VNE and QFI of Three-Level Moving Stark Shifted Atomic Systems under the Influence of NLKM

#### Explanation of Graphs

FIG-3 This graph depicts the behavior of QFI and VNE as a function of time under different conditions of the Kerr nonlinearity parameter  $\chi = 0.3, 1$  and  $3$  and the phase  $\phi = 0, \phi = \pi/4$ . The

key features are influenced by atomic motion, the Stark effect parameter  $\beta = 0.3$ , and QE in NLKM. (a) QFI for  $\theta = 0$  and (b) QFI for  $\theta = \pi/4$ : QFI measures the sensitivity of a quantum state to changes in a parameter and is directly related to the precision of quantum measurements. Higher QFI values imply better precision. For  $\chi = 0.3$  (red line), QFI shows periodic oscillations with sharp dips, indicating significant influence of the NLKM and atomic motion. For  $\chi = 1$  (blue line) and  $\chi = 3$  (green line), QFI stabilizes at high values, reflecting lesser sensitivity to the atomic motion or nonlinear effects. (c)

VNE for  $\theta = 0$  and (d) VNE for  $\theta = \pi/4$ : VNE quantifies QE, with higher values indicating stronger QE. The red line ( $\chi = 0.3$ ) exhibits pronounced oscillations in VNE, showing strong variations in QE over time, corresponding to periodic coupling between subsystems mediated by the NLKM and atomic motion. For  $\chi = 1$  and  $\chi = 3$ , VNE remains relatively low, indicating weaker QE. The oscillatory behavior in both QFI and VNE, especially for  $\chi = 0.3$ , is indicative of dynamic interactions between atomic motion and the NLKM. This motion induces periodic modulations in QE and precision QFI, particularly at low  $\chi$ . QE plays a pivotal role in enhancing QFI. Peaks in QFI often align with dips in VNE, suggesting a trade-off between the precision of parameter estimation.

FIG-4 Atoms in this system are coupled to a nonlinear medium (Kerr medium) and experience periodic dynamics. The motion could correspond to oscillations between energy levels due to Rabi cycling or interactions with an external field. These oscillations are reflected in the QFI and VNE's periodic nature. The atomic motion drives transitions between different quantum states, affecting coherence (QFI) and entanglement (VNE). The NLKM  $\chi = 0.3$  introduces a non-linear term into the Hamiltonian, meaning that the interaction strength between the atoms depends on their quantum state. This non-linearity leads to state-dependent phase shifts that influence the atomic dynamics. Imagine that the atomic system is in a cavity where the non-linearity of the medium bends the "optical paths" of the atoms in a way that depends on their quantum states.

This bending causes oscillatory behavior in the quantum coherence and QE. The oscillations in QFI and VNE emerge from the interplay between the Kerr-induced non-linearity and the periodic atomic motion. QFI as a Measure of Coherence: QFI reflects how much information about a parameter (like  $\theta$ ) can be extracted from the quantum state. A high QFI indicates strong coherence and sensitivity to external parameters. High QFI values ( $>0.96$ ): The system is largely coherent, meaning the quantum state retains well-defined phase relationships. Periodic Dips: As the atomic motion evolves, interactions in the Kerr medium and external fields periodically modulate the state coherence, causing temporary reductions in QFI.

Phase Dependence ( $\theta = 0$  vs.  $\theta = \pi/4$ ): Changing  $\theta$  adjusts the interference pattern of the atomic wavefunctions, slightly shifting the oscillations. VNE quantifies the QE or mixedness of the system. If the entropy is low (close to zero), the system is in a pure state; higher values indicate more QE or decoherence. Low QE ( $\approx 0.1$ ): The system is predominantly in a pure quantum state, suggesting minimal interaction between subsystem. The spikes in VNE correspond to moments when the atomic motion and

non-linear interactions temporarily increase QE between different parts of the system (e.g., between atomic internal states or field modes in the Kerr medium). The Stark effect  $\beta = 0.3, 1$  and  $3$  shifts atomic energy levels due to an external electric field.

The parameter  $\beta$  quantifies the strength of this shift. Physically,  $\beta$  modifies the time evolution of the system by introducing energy level differences. Small  $\beta = 0.3$ : The energy shifts are small, so the atomic motion and coherence oscillations are less disturbed. This results in smoother dynamics, as seen in the red curves. Large  $\beta = 3$ : Higher Stark shifts introduce stronger energy level splitting, leading to faster and sharper oscillations in both QFI and VNE. The green curves reflect these more pronounced dynamics. The atomic system evolves under the competing influences of the Kerr medium's non-linearity and the Stark effect. Physically, this is akin to a pendulum swinging in a medium that changes its properties depending on the pendulum's state. The high QFI indicates the pendulum's motion remains regular and predictable, making the system highly sensitive to phase or energy shifts.

Small spikes in VNE represent transient moments when the pendulum's motion briefly entangles with other degrees of freedom, such as the medium or another pendulum. Changing  $\theta$  adjusts the initial conditions of the system's dynamics, similar to starting a pendulum swing from different angles. In the graphs at  $\theta = 0$ : the oscillations appear slightly simpler and more symmetric.  $\theta = \pi/4$ , a phase offset introduces subtle asymmetries or shifts in the oscillation patterns of QFI and VNE. Atomic motion: Drives periodic coherence and QE dynamics. NLKM medium ( $\chi = 0.3$ ) introduces non-linearity, leading to periodic modulation of quantum properties.

The SE  $\beta$  alters energy levels, influencing the amplitude and frequency of the oscillations. QFI shows high coherence, suitable for quantum metrology. VNE: Shows minimal QE, indicating a predominantly pure state with transient increases in QE. This interplay demonstrates a quantum system where coherence dominates, with QE emerging briefly during atomic motion cycles. The physical system is highly controllable via  $\beta$ ,  $\chi$ , and  $\theta$ , making it ideal for precision quantum sensing or fundamental studies of quantum dynamics.

## Conclusion

The study investigates the behavior of QFI and VNE in three-level stationary and moving Stark-shifted atomic systems coupled with a nonlinear Kerr medium. QFI, representing quantum coherence and sensitivity, decreases over time due to decoherence but stabilizes for higher Kerr nonlinearity values. VNE, a measure of quantum entanglement, increases over time, with stronger growth observed for lower nonlinearity values, reflecting enhanced entanglement. The Stark effect introduces energy level shifts that modulate quantum state dynamics, leading to oscillatory behavior in both QFI and VNE. The phase parameter influences these oscillations, with symmetric patterns at one phase value and more complex dynamics at another.

In the moving systems, the atomic motion interacts with the nonlinear medium and the Stark effect, creating periodic oscillations in QFI and VNE. For lower Kerr nonlinearity values, these oscillations are more pronounced, indicating a stronger impact



of nonlinear interactions and motion on coherence and entanglement. Higher nonlinearity values stabilize QFI, while VNE exhibits reduced fluctuations, indicating weaker entanglement. The Stark effect significantly affects the oscillation amplitude and frequency, with stronger energy shifts leading to sharper fluctuations. Changes in the phase parameter further modulate interference patterns and the evolution of QFI and VNE.

Peaks in QFI often align with dips in VNE, suggesting a trade-off between coherence and entanglement. The interplay of Kerr nonlinearity, Stark effect, and phase provides a controllable framework for managing quantum properties such as coherence and entanglement. Lower nonlinearity values enhance entanglement, while higher values preserve coherence, making these systems suitable for precision quantum metrology. The ability to control the system parameters allows for tailored quantum systems designed for applications in sensing, quantum computing, and studies of fundamental quantum dynamics.

## References

1. Hore, B. W., & Knight, P. L. (1993). The Jaynes-Cummings model. *Journal of Modern Optics*, 40(7), 1195–1238.
2. Alqannas, H. S., & Abdel-Khalek, S. (2019). Nonclassical properties and field entropy squeezing of the dissipative two-photon JCM under Kerr like medium based on dispersive approximation. *Optics & Laser Technology*, 111, 523–529.
3. Rempe, G., Walther, H., & Klein, N. (1987). Observation of quantum collapse and revival in a one-atom maser. *Physical Review Letters*, 58(4), 353.
4. Yoo, H.-I., & Eberly, J. H. (1985). Dynamical theory of an atom with two or three levels interacting with quantized cavity fields. *Physics Reports*, 118(5), 239–337.
5. Li, X.-s., & Lin, D. L. (1987). Nonresonant interaction of a three-level atom with cavity fields. I. General formalism and level occupation probabilities. *Physical Review A*, 36(11), 5209.
6. Abdel-Hafez, A. M., Obada, A. S. F., & Ahmad, M. M. A. (1987). N-level atom and (N–1) modes generalized models and multiphons. *Physica A: Statistical Mechanics and its Applications*, 144(2-3), 530–560.
7. Abdel-Hafez, A. M., Obada, A.-S. F., & Ahmad, M. M. A. (1987). N-level atom and (N–1) modes: An exactly solvable model with detuning and multiphotons. *Journal of Physics A: Mathematical and General*, 20(6), L359.
8. Abdel-Hafez, A. M., Abu-Sitta, A. M. M., & Obada, A.-S. F. (1989). A generalized Jaynes-Cummings model for the N-level atom and (N–1) modes. *Physica A: Statistical Mechanics and its Applications*, 156(2), 689–712.
9. Abdel-Aty, M. (2001). Entanglement degree of a three-level atom interacting with pair-coherent states with a nonlinear medium. *Laser Physics*, 11(7), 871–878.
10. Obada, A. S. F., Hanoura, S. A., & Eied, A. A. (2013). Entanglement for a general formalism of a three-level atom in a V-configuration interacting nonlinearly with a non-correlated two-mode field. *Laser Physics*, 23(5), 055201.
11. Abdel Wahab, N. H., & Salah, A. (2015). A novel solution procedure for a three-level atom interacting with one-mode cavity field via modified homotopy analysis method. *The European Physical Journal Plus*, 130(5), 92.
12. Abd El-Wahab, N. H., & Salah, A. (2015). The influence of the classical homogenous gravitational field on interaction of a three-level atom with a single mode cavity field. *Modern Physics Letters B*, 29(29), 1550175.
13. Liu, J.-r., & Wang, Y.-z. (1996). Velocity-selective population and quantum collapse-revival phenomena of the atomic motion for a motion-quantized Raman-coupled Jaynes-Cummings model. *Physical Review A*, 54(3), 2444.
14. Faghihi, M. J., Tavassoly, M. K., & Hatami, M. (2014). Dynamics of entanglement of a three-level atom in motion interacting with two coupled modes including parametric down conversion. *Physica A: Statistical Mechanics and its Applications*, 407, 100–109.
15. Zait, R. A., & Abd El-Wahab, N. H. (2002). Nonresonant interaction between a three-level atom with a momentum eigenstate and a one-mode cavity field in a Kerr-like medium. *Journal of Physics B: Atomic, Molecular and Optical Physics*, 35(17), 3701.
16. Osman, M. S., & Abdel-Gawad, H. I. (2015). Multi-wave solutions of the (2+1)-dimensional Nizhnik-Novikov-Veselov equations with variable coefficients. *The European Physical Journal Plus*, 130, 1–11.
17. Bartlett, R. (2023). Alternating current and superconductivity quantum entanglement of waves replaces nuclear fusion as the power source in stars. SSRN. <https://ssrn.com/abstract=4556339>
18. Feng, T., Song, Z., Wu, T., Lu, X., & Li, L. (2023). Quantum entanglement source model pumped by low-power laser diode. In *Conference on Infrared, Millimeter, Terahertz Waves and Applications (IMT2022)* (Vol. 12565, pp. 362–370). SPIE.
19. Sun, W.-Y., Wang, D., Fang, B.-L., & Ye, L. (2018). Quantum dynamics characteristic and the flow of information for an open quantum system under relativistic motion. *Laser Physics Letters*, 15(3), 035203.
20. Goradia, S. G. (2019). The quantum theory of entanglement and Alzheimer's. *Journal of Alzheimer's & Neurodegenerative Diseases*, 5, 01–03.
21. Little, D. (2018). Entangling the social: Comments on Alexander Wendt, quantum mind and social science. *Journal of Theory of Social Behaviour*, 48(2), 167–176.
22. Bhattacharyya, S., Das, A., Banerjee, A., & Chakrabarti, A. (2023). Comparative study of noises over quantum key distribution protocol. In S. Bhattacharyya (Ed.), *International Conference on Data Management, Analytics & Innovation* (pp. 759–782). Springer.
23. Lee, J. Y., You, Y.-Z., & Xu, C. (2022). Symmetry protected topological phases under decoherence. *arXiv preprint arXiv:2210.16323*.
24. Khalid, U., Jeong, Y., & Shin, H. (2018). Measurement-based quantum correlation in mixed-state quantum metrology. *Quantum Information Processing*, 17, 1–12.
25. Triggiani, D., Facchi, P., & Tamma, V. (2022). The role of auxiliary stages in Gaussian quantum metrology. *Photonics*, 9, 345.
26. Apellaniz, I., Kleinmann, M., Gühne, O., & Tóth, G. (2017). Optimal witnessing of the quantum Fisher information with few measurements. *Physical Review A*, 95(3), 032330.
27. Beckey, J. L., Cerezo, M., Sone, A., & Coles, P. J. (2022). Variational quantum algorithm for estimating the quantum Fisher information. *Physical Review Research*, 4(1), 013083.



28. Rath, A., Branciard, C., Minguzzi, A., & Vermersch, B. (2021). Quantum Fisher information from randomized measurements. *Physical Review Letters*, 127(26), 260501.
29. Li-Yun, H., Rao, Z.-M., & Kuang, Q.-Q. (2019). Evolution of quantum states via Weyl expansion in dissipative channel. *Chinese Physics B*, 28(8), 084206.
30. Naikoo, J., Banerjee, S., & Srikanth, R. (2021). Quantumness of channels. *Quantum Information Processing*, 20, 1–11.
31. Falaye, B. J., et al. (2017). Investigating quantum metrology in noisy channels. *Scientific Reports*, 7(1), 16622.
32. Xiong, W., Jin, D.-Y., Qiu, Y., Lam, C.-H., & You, J. Q. (2016). Cross-Kerr effect on an optomechanical system. *Physical Review A*, 93, 023844.
33. Chen, J., Fan, X.-G., Xiong, W., Wang, D., & Ye, L. (2023). Nonreciprocal entanglement in cavity-magnon optomechanics. *Physical Review B*, 108, 024105.
34. Zhang, D., & Zheng, Q. (2013). Enhancing stationary optomechanical entanglement with the Kerr medium. *Chinese Physics B*, 22, 064206.
35. Pagel, D., Alvermann, A., & Fehske, H. (2016). Dynamic Stark effect, light emission, and entanglement generation in a laser-driven quantum optical system. *arXiv preprint arXiv:1609.03788*.
36. Anwar, S. J., Ramzan, M., & Khan, M. K. (2019). Effect of Stark- and Kerr-like medium on the entanglement dynamics of two three-level atomic systems. *Quantum Information Processing*, 18, 192.
37. Abdel-Khalek, S. (2013). Quantum Fisher information for moving three-level atom. *Quantum Information Processing*, 12, 3761.
38. Lu, X., Wang, X., & Sun, C. P. (2010). Quantum Fisher information flow and non-Markovian processes of open systems. *Physical Review A*, 82, 042103.
39. Barndorff-Nielsen, O. E., Gill, R. D., & Jupp, P. E. (2003). On quantum statistical inference. *Journal of the Royal Statistical Society: Series B (Statistical Methodology)*, 65, 775–816.